

# Deployment and Retrieval Optimization of a Tethered Satellite System

Ehud Netzer\*

*Technion—Israel Institute of Technology, Haifa 32000, Israel*  
and

Thomas R. Kane†

*Stanford University, Stanford, California 94305*

This paper describes the optimization analysis results of deployment and retrieval of a tethered satellite system. The system is composed of two small satellites connected by a long tether. One of the satellites is equipped with a set of thrusters for purposes of control. The optimization analysis is based on the nonlinear equations of motion, and the optimized length law together with the optimized thrust histories are calculated. The optimization is performed with a MATLAB-based multicontroller algorithm. First, the algorithm is used to optimize the phases of deployment and retrieval for a simple model where the tether is represented by a massless rod. Then these results are used as a nominal path for a retrieval involving a more realistic model. When this model is used to simulate retrieval, the system is kept on the nominal path by means of a regulator. The optimization result, compared with results in previous papers, points to improved performance and a significant reduction in fuel consumption.

## Introduction

THE system under consideration consists of two tether-connected, unmanned satellites of approximately the same mass.<sup>1</sup> One of the satellites is equipped with scientific instruments, the other with a reel and a set of thrusters for control purposes. The problem of optimizing deployment and retrieval of the primary satellite may be stated as follows: What are the length laws and thrust histories to perform deployment and retrieval in such a way that a given performance index is minimized? A survey of the literature on tether systems shows that even though deployment and retrieval are the most critical phases of such missions, and have been the subject of most analyses,<sup>2,3</sup> only limited attention has been devoted to the optimization problem.

Because optimized length laws are part of the product of this paper, we present various length laws that have been used in previous work. In most control strategies, the tension in the tether or the length rate are functions of a reference length and of the swing angles.<sup>2</sup> Thus, the actual length history is a result of the control law rather than being prescribed. The reference length, on the other hand, is assigned by the designer, and it can have a fixed value, for example, that of the final length,<sup>4,5</sup> or it may change exponentially, so that the length rate is small when the tether is short.<sup>6,7</sup> When thrusters are used as controllers, one can specify the actual length. Xu et al.<sup>8</sup> and later Lakshmanan et al.<sup>9</sup> used an exponential law for the prescribed length law. A paper that addresses the issue of trajectory optimization was presented by Fleurisson et al.<sup>10</sup> In this paper, the authors calculate the optimal length law to deploy and retrieve a satellite from the Shuttle, and use feedforward and feedback control to keep the system on this path. The optimization is based on the length-rate control strategy, which leads to pitch angles as large as 1 rad. It is assumed that the Shuttle moves on a circular orbit and the optimization results are not checked with a massive tether model.

An approximation usually made in the design of a controller for deployment and retrieval is the linearization of equations of motion.<sup>1,6,11,12</sup> This is required to enable one to use linear control tools, such as linear quadratic regulator (LQR) theory. In a general optimization algorithm, such as the one used in this paper, the state histories can be found through the relation

$$\dot{x} = f[x(t), v(t), t], \quad x(0) = x_0 \quad (1)$$

where  $f$  is a set of nonlinear functions of the state vector  $x$ , the control vector  $v$ , and time. Some nonlinear terms are found to be significant and must be included in the analysis; other nonlinear terms were found to be more than two orders of magnitude smaller.

For comparison, we include results obtained by the linear approach, by which we mean that a length law is prescribed, the equations of motion are linearized with respect to states

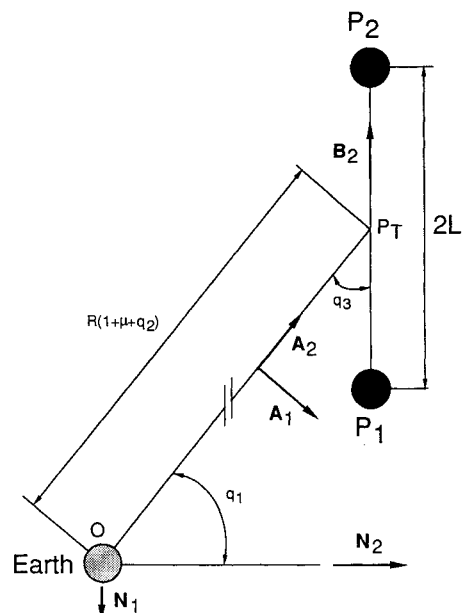


Fig. 1 Simple model for optimization.

Received May 14, 1992; revision received Oct. 5, 1992; accepted for publication Nov. 27, 1992. Copyright © 1993 by E. Netzer and T. R. Kane. Published by the American Institute of Aeronautics and Astronautics, Inc., with permission.

\*Adjunct Teaching Fellow, Faculty of Mechanical Engineering.

†Professor of Applied Mechanics.

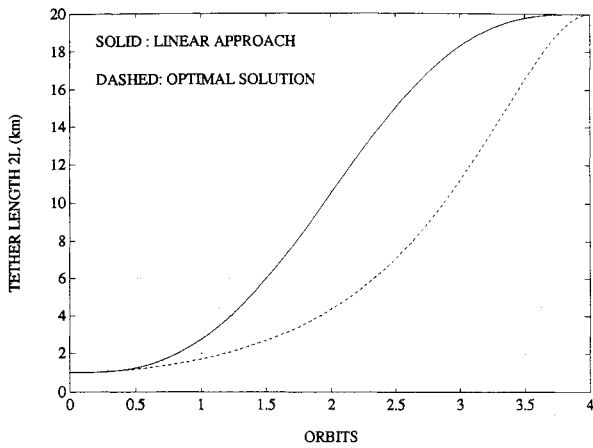


Fig. 2 Optimization results for deployment: comparison of length laws.

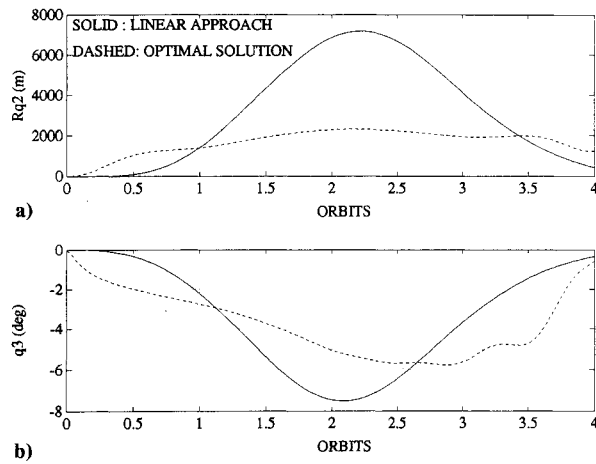


Fig. 3 Optimization results for deployment: comparison of state histories; a) range deviation  $Rq_2$  (m) and b) swing angle  $q_3$  (deg).

and controllers, and the LQR technique is used to design the feedback gains.<sup>1</sup> The prescribed length law that is used for the linear approach is presented graphically in Figs. 2 and 5.

The purpose in this paper is to find the optimized length law and thrust histories such that deployment and retrieval are accomplished in a given time while a specified performance index is minimized. A MATLAB-based<sup>13</sup> multicontroller algorithm<sup>14</sup> has been formulated and used. It is based on the Mayer formulation<sup>15</sup> in which the performance index is treated as an additional state variable.

### Model Description and System Equations

The analytical model is depicted in Fig. 1. The two satellites are modeled as particles  $P_1$  and  $P_2$ , each of mass  $M$ , and the tether is modeled as a straight, massless object  $S$  of length  $2L$ . Two thrusters are located on  $P_2$ , one aligned with and the other perpendicular to the tether. The system is presumed to be in the gravitational field of a particle  $O$  of mass  $M_E$  (the mass of the Earth) that is fixed in a Newtonian reference frame  $N$ . Because out-of-plane motion is well controlled with little effort,<sup>1</sup> the model is planar, and only in-plane motion is considered.

To characterize the behavior of the system, we begin by introducing constants  $G_E$ ,  $\Omega$ , and  $R$ .  $G_E$  is the universal gravitational constant, and  $\Omega$  is the orbital rate at which a particle in the gravitational field of  $O$  moves on a circular orbit of radius  $R$ , so that

$$R = (G_E M_E / \Omega^2)^{1/3} \quad (2)$$

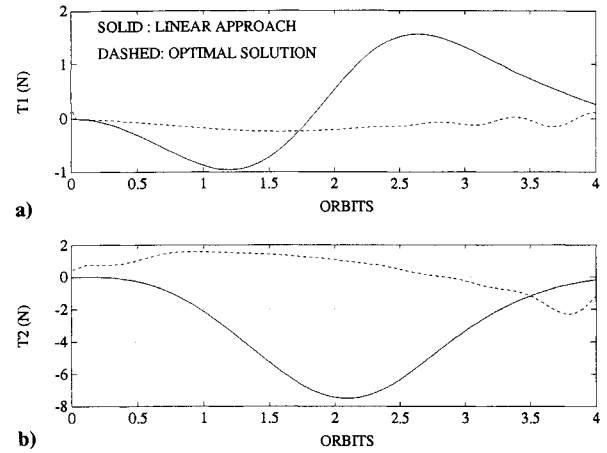


Fig. 4 Optimization results for deployment: comparison of thrust histories (N); a)  $T_1$  and b)  $T_2$ .

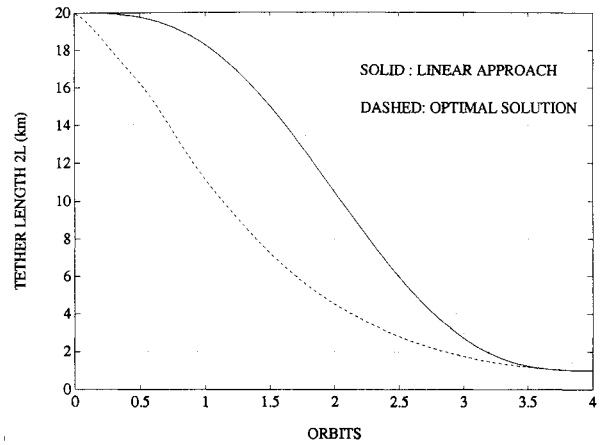


Fig. 5 Optimization results for retrieval: comparison of length laws.

Next, because the system possesses three degrees of freedom in  $N$ , we define generalized coordinates  $q_i$  ( $i = 1, 2, 3$ ) in conjunction with establishing a number of vector bases. The first of these is a dextral set of mutually perpendicular unit vectors  $N_i$  ( $i = 1, 2, 3$ ) fixed in  $N$  (see Fig. 1), with  $N_3$  normal to the plane in which the system is intended to move. We align unit vectors  $A_i$  with  $N_i$  ( $i = 1, 2, 3$ ) and subject the former triad to a dextral rigid-body rotation of amount  $q_1$  about  $N_3$ . In addition, we require that the tether midpoint  $P_T$  lies at all times on the line that passes through  $O$  and is parallel to  $A_2$ ; also, we let  $q_2$  be a dimensionless coordinate, and  $\mu$  a dimensionless quantity, such that  $r^{O-P_T}$ , the position vector from  $O$  to  $P_T$ , is given by

$$r^{O-P_T} = R(1 + \mu + q_2)A_2 \quad (3)$$

The motion that occurs when  $q_2$  vanishes,  $\dot{q}_1 = \Omega$ , and the tether is parallel to  $A_2$ , is called the *desired motion* of the system. Because  $P_1$  and  $P_2$  have the same mass, the value of  $\mu$  is of the order of  $10^{-6}$  and is neglected during the optimization.

To orient the tether relative to  $A_i$  ( $i = 1, 2$ ), we attach reference frame  $B$  to  $S$ , let  $B_i$  ( $i = 1, 2, 3$ ) be unit vectors fixed in  $B$ , align  $B_i$  with  $A_i$  ( $i = 1, 2, 3$ ), and subject  $B$  to a rotation characterized by the vector  $q_3 A_3$ .

In terms of a dimensionless quantity  $\tau$  defined as

$$\tau = \Omega t \quad (4)$$

the kinematical differential equations for the generalized speeds  $u_1, u_2, u_3$  can be written

$$u_1 = \frac{dq_1}{d\tau} - 1, \quad u_i = \frac{dq_i}{d\tau} \quad i = 2, 3 \quad (5)$$

In addition to gravitational forces exerted by  $O$  on  $P_1$  and  $P_2$ , the analytical model is to accommodate control forces exerted on  $P_2$  by means of thrusters. To this end, we introduce a thrust vector  $T$  as

$$T = T_1 B_1 + T_2 B_2 \quad (6)$$

$T_1$  and  $T_2$  are functions of system states, chosen on the basis of control theory in such a way to keep the system near the required orientation.

The equations of motion, omitted in the interest of brevity, are generated with Autolev.<sup>16</sup> These equations are nonlinear and coupled; and they include time-dependent terms when deployment and retrieval are in progress. For optimization, the equations are simplified so that they include all linear terms, but only the most significant nonlinear ones.

For control design, it is desirable that the states and controllers be balanced, which means that they are scaled in such a way that the significance of each one is of the same order of magnitude. With this in mind, we introduce the scaled generalized coordinates, generalized speeds, and controllers (designated by a caret), together with a number of constants and variables as follows:

$$\alpha_f = L_f / R \quad (7)$$

$$\bar{L} = L / L_f \quad (8)$$

$$\Lambda' = L' / L \quad (9)$$

$$\hat{u}_i = u_i / \alpha_f \quad i = 1, 2, \quad \hat{u}_3 = 10u_3 \quad (10)$$

$$\hat{q}_2 = q_2 / \alpha_f, \quad \hat{q}_3 = 10q_3 \quad (11)$$

$$\hat{T}_i = T_i / (ML_f \Omega^2) \quad i = 1, 2 \quad (12)$$

where  $L_f$  is the tether half-length when the tether is fully deployed, and prime denotes differentiation with respect to  $\tau$ . The simplified equations of motion are

$$\hat{u}_1' = -2\hat{u}_2 + 0.3\alpha_f \bar{L}^2 \hat{q}_3 - 0.5(1 + \alpha_f \hat{q}_2) \hat{T}_1 + 0.05 \hat{q}_3 \hat{T}_2 \quad (13)$$

$$\hat{u}_2' = 3\hat{q}_2 + 2\hat{u}_1 + 0.5 \hat{T}_2 + 0.05 \hat{q}_3 \hat{T}_1 \quad (14)$$

$$\begin{aligned} \hat{u}_3' = & 20\alpha_f \hat{u}_2 - 20\Lambda'(1 + \alpha_f \hat{u}_1 + 0.1\hat{u}_3) - 3\hat{q}_3 \\ & + 5[-(1/\bar{L}) + \alpha_f + \alpha_f^2 \hat{q}_2] \hat{T}_1 - 0.5\alpha_f \hat{q}_3 \hat{T}_2 \end{aligned} \quad (15)$$

It should be noted that the nonlinear terms in Eqs. (13–15) include products of states and thrusts. These are found to be the dominant nonlinear terms, whereas the other nonlinear terms are more than two orders of magnitude smaller.

The term  $\Lambda'$ , which describes the normalized length rate, can be regarded either as a state or as a controller. If it is used as a state, its initial value must be specified and a constraint may be imposed on its terminal value. In such a formulation, the control is composed of the second derivative of the tether length, and the numerical solution is less robust relative to the other formulation, in which  $\Lambda'$  is a controller. The advantages of both approaches are incorporated in our final decision:  $\Lambda'$  is considered as a controller in the first runs, which enables us to use the less sensitive version when we are not yet familiar with the nature of the solution; and the results from this version are used as initial guesses for the second version, where  $\Lambda'$  is considered as a state.

## Performance Index

The performance index to be minimized is

$$J = a_1[\hat{q}_2(\tau_f)]^2 + a_2[\hat{u}_2(\tau_f)]^2 + a_3[\hat{q}_3(\tau_f)]^2 + a_4[\hat{u}_3(\tau_f)]^2 + J_a \quad (16)$$

where

$$\begin{aligned} J_a = & \int_{\tau=0}^{\tau_f} \{b_1[\hat{u}_1(\tau)]^2 + b_2[\hat{q}_2(\tau)]^2 + b_3[\hat{u}_2(\tau)]^2 + b_4[\hat{q}_3(\tau)]^2 \\ & + b_5[\hat{u}_3(\tau)]^2 + b_6[\hat{T}_1(\tau)]^2 + b_6[\hat{T}_2(\tau)]^2\} d\tau \end{aligned} \quad (17)$$

This performance index involves penalties on the terminal values of the states as well as on the states and controllers throughout the maneuver. Based on the system parameters given later, the weights, chosen by means of an iterative process, are

$$a_1 = 45, \quad a_2 = 300, \quad a_3 = a_4 = 15$$

$$b_1 = b_2 = b_3 = 1, \quad b_4 = b_5 = 1.8, \quad b_6 = 1 \quad (18)$$

The values for  $a_1, a_2$ , and  $a_3$  were set iteratively, whereas the values for  $b_i$  ( $i = 1, \dots, 5$ ), interpreted in terms of physical units, indicate our willingness to use 1.1 N of thrust for a range deviation of 2500 m and a swing angle of 0.9 deg. These relations indicate the relative importance of the various states and controls.

## $\Lambda'$ as a Controller

When  $\Lambda'$  is considered as a controller, the state vector is

$$\mathbf{x} = [x_1, \dots, x_7] = [\hat{u}_1 \ \hat{q}_2 \ \hat{u}_2 \ \hat{q}_3 \ \hat{u}_3 \ \bar{L} \ J_a]^T \quad (19)$$

and the control vector is

$$\mathbf{v} = [v_1, v_2, v_3] = [\hat{T}_1 \ \hat{T}_2 \ \Lambda']^T \quad (20)$$

With these substitutions, we write Eqs. (13–15) as five first-order differential equations and add two differential equations for the length and the performance index to obtain

$$x_1' = -2x_3 + 0.3\alpha_f x_6^2 x_4 - 0.5(1 + \alpha_f x_2)v_1 + 0.05x_4 v_2 \quad (21)$$

$$x_2' = x_3 \quad (22)$$

$$x_3' = 3x_2 + 2x_1 + 0.5v_2 + 0.05x_4 v_1 \quad (23)$$

$$x_4' = x_5 \quad (24)$$

$$\begin{aligned} x_5' = & 20\alpha_f x_3 - 20u_3(1 + \alpha_f x_1 + 0.1x_5) - 3x_4 \\ & + 5(-1/x_6 + \alpha_f + \alpha_f^2 x_2)v_1 - 0.5\alpha_f x_4 v_2 \end{aligned} \quad (25)$$

$$x_6' = v_3 x_6 \quad (26)$$

$$x_7' = b_1 x_1^2 + b_2 x_2^2 + b_3 x_3^2 + b_4 x_4^2 + b_5 x_5^2 + b_6(v_1^2 + v_2^2) \quad (27)$$

## $\Lambda'$ as a State

When  $\Lambda'$  is considered as a state, an extra state is added to Eq. (19), which leads to

$$\mathbf{x} = [x_1, \dots, x_8] = [\hat{u}_1 \ \hat{q}_2 \ \hat{u}_2 \ \hat{q}_3 \ \hat{u}_3 \ \bar{L} \ \Lambda' \ J_a]^T \quad (28)$$

and the new control vector is

$$\mathbf{v} = [v_1, v_2, v_3] = [\hat{T}_1 \ \hat{T}_2 \ \Sigma']^T \quad (29)$$

where

$$\Sigma' = L'' / L \quad (30)$$

With these substitutions, the seven differential equations (21–27) are replaced with the following eight equations:

$$x_1' = -2x_3 + 0.3\alpha_f x_6^2 x_4 - 0.5(1 + \alpha_f x_2)v_1 + 0.05x_4 v_2 \quad (31)$$

$$x_2' = x_3 \quad (32)$$

$$x_3' = 3x_2 + 2x_1 + 0.5v_2 + 0.05x_4 v_1 \quad (33)$$

$$x_4' = x_5 \quad (34)$$

$$x_5' = 20\alpha_f x_3 - 20x_7(1 + \alpha_f x_1 + 0.1x_5) - 3x_4 + 5(-1/x_6 + \alpha_f + \alpha_f^2 x_2)v_1 - 0.5\alpha_f x_4 v_2 \quad (35)$$

$$x_6' = x_6 x_7 \quad (36)$$

$$x_7' = v_3 - x_7^2 \quad (37)$$

$$x_8' = b_1 x_1^2 + b_2 x_2^2 + b_3 x_3^2 + b_4 x_4^2 + b_5 x_5^2 + b_6(v_1^2 + v_2^2) \quad (38)$$

### Optimization Description and Results

#### Initial States and Terminal Constraints

When  $\Lambda'$  is used as a controller, the initial state vector for deployment is

$$x(0) = [0 \ 0 \ 0 \ 0 \ 0 \ 0.05 \ 0]^T \quad (39)$$

For retrieval, it is

$$x(0) = [0 \ 0 \ 0 \ 0 \ 0 \ 1 \ 0]^T \quad (40)$$

The terminal constraint for deployment is

$$x_6(\tau_f) = L(\tau_f)/L_f = 1 \quad (41)$$

and for retrieval is

$$x_6(\tau_f) = L(\tau_f)/L_f = 0.05 \quad (42)$$

The shortest length of the tether is 5% of the full length because length rate and length acceleration are normalized by the actual length, so that the optimization algorithm is very sensitive to changes in the control vector when the tether is very short. This sensitivity may be overcome by using smaller gains in the optimization algorithm, and thus, significantly increasing the run time. The deployment and retrieval of the last 5% can be accomplished by using any prescribed length law.

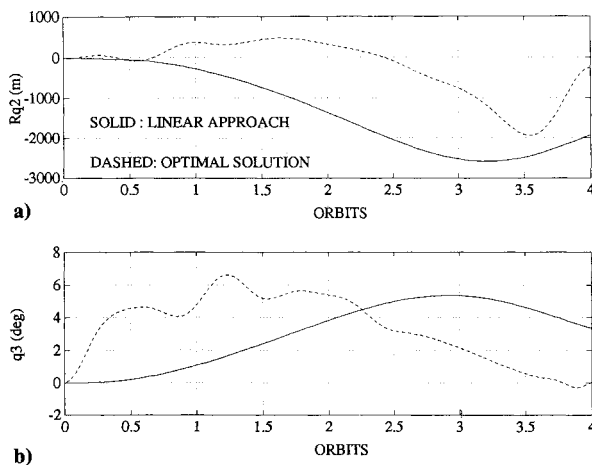


Fig. 6 Optimization results for retrieval: comparison of state histories; a) range deviation  $Rq_2$  (m) and b) swing angle  $q_3$  (deg).

When  $\Lambda'$  is considered as a state, its initial value must be specified, and a constraint may be imposed on its terminal value. Because of the small time constants of the system relative to the time constant of the reel motor, we may use a nonzero initial value for  $\Lambda'$  for retrieval, but it is important to have a zero terminal value, so that the satellites do not move toward each other at the end of the maneuver. Consequently, the initial vector for deployment is taken to be

$$x(0) = [0 \ 0 \ 0 \ 0 \ 0 \ 0.05 \ 0]^T \quad (43)$$

For retrieval, we use

$$x(0) = [0 \ 0 \ 0 \ 0 \ 0 \ 1 \ -0.04 \ 0]^T \quad (44)$$

An additional terminal constraint, corresponding to  $\Lambda'(\tau_f)$ , is added to Eqs. (41) and (42), namely

$$x_7(\tau_f) = \Lambda'(\tau_f) = 0 \quad (45)$$

#### Initial Guess of the Controller

The optimization algorithm is formulated to find a local minimum. Hence it is important to have some knowledge about the final solution so that a good initial guess for the control histories can be made. When  $\Lambda'$  is considered as a controller, two sets of initial guesses are used. The first includes the results from the linear approach with the prescribed length law, and the second is an all-zero state vector. The optimization results for the two cases are very similar, which leads to the presumption that it is a global minimum. The optimized solution with this formulation furnishes initial guesses for the next step, where  $\Lambda'$  is considered as a state.

#### Optimization Results

The optimization results for deployment are shown in Figs. 2–4, and for retrieval in Figs. 5–7. The figures also show, for comparison, the results obtained by using the linearized equations of motion and a prescribed length law (Fig. 2).

For the simulation, we take  $M = 500$  kg,  $L_f = 10$  km (total tether length of 20 km),  $t_f = 21,342$  s = 4 orbits,  $R = 6.598388 \times 10^6$  m, and  $\Omega = 1.178486395 \times 10^{-3}$  rad/s.

#### Deployment

Figure 2 shows the comparison between the optimal solution and the prescribed law that is used for the linear model. The prescribed law is a symmetric function whose first and second time derivatives vanish at the beginning and at the conclusion of the maneuver. In the optimal solution, the length changes slowly in the beginning (when the tether is

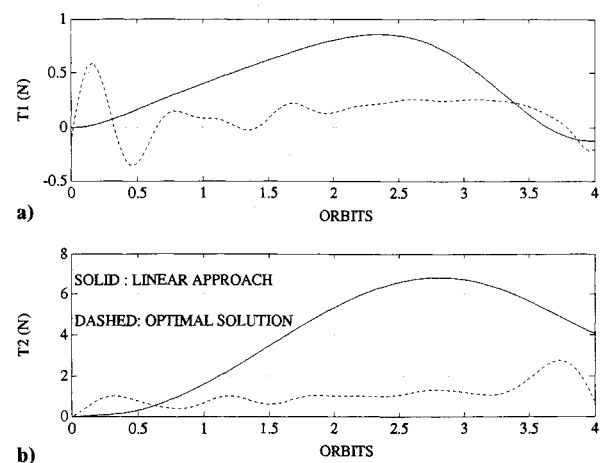


Fig. 7 Optimization results for retrieval: comparison of thrust histories (N); a)  $T_1$  and b)  $T_2$ .

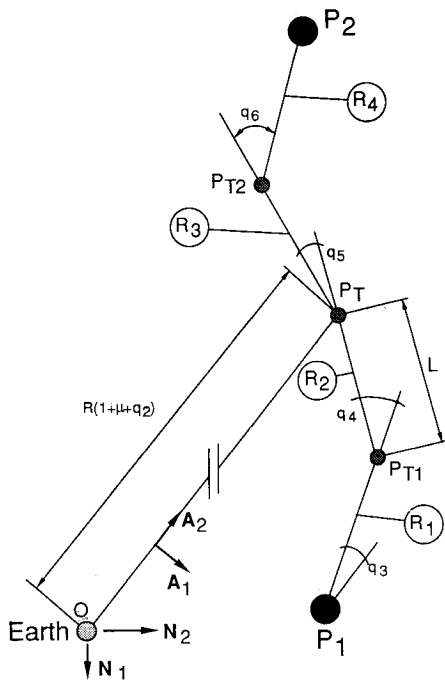


Fig. 8 Six-degree-of-freedom model.

short), and more rapidly when the tether is longer. This kind of solution assures positive tension in the tether (even though it was not a design criterion). Figure 3 shows the state histories; the maximum range deviation from the nominal orbit radius is 2200 m for the optimal solution vs 7100 m for the linear approach (Fig. 3a); the maximum value of  $q_3$  is 5.6 deg for the optimal solution and 7.7 deg for the linear approach (Fig. 3b). The most significant improvement is shown in Fig. 4, where the thrust histories for the two cases are compared. The maximum thrusts for the optimal solution are 0.25 and 2.2 N for  $T_1$  and  $T_2$ , respectively, whereas they are 1.6 and 7.7 N, respectively, for the linear model. It is interesting to note that, whereas  $T_2$  is negative for the linear model, it is mainly positive for the optimal solution. The nonlinear equations (21–26) and (31–36) include products of thrusts and generalized coordinates that are neglected in the linear approach. These terms are found to have the same order of magnitude as the thrust linear terms. Hence, while the thrust components “fight” one another in the linear approach, their action is coordinated in the optimal solution, and fuel is used more efficiently.

The total performance index for deployment is 25.2 units for the optimal solution, whereas it is 42.5 units for the linear model—an improvement of 40%. Most of the improvement is achieved by using much less thrust, i.e., 0.7 units are related to thrust usage for the optimal solution in contrast with 9.0 units for the linear model. In terms of fuel consumption, the linear solution requires 21.2 kg of fuel whereas the optimal solution requires only 1.65 kg. It is interesting to note that the improvement due to the new length law is about 21% (out of the total 40%), and the rest is due to the use of nonlinear terms in the equations and, thus, the coordinated action of the thrusts.

#### Retrieval

The results for the retrieval are presented in Figs. 5–7. Figure 5 shows the optimal length law together with the prescribed law used for the linear model. As in the case of deployment, the length rate is higher when the tether is longer. The state histories are shown in Fig. 6; the terminal values for both  $Rq_2$  and  $q_3$  are much smaller for the optimal solution than for the linear model (Figs. 6a and 6b) due to the penalties on these values. The maximum value for  $q_3$  is 6.7 deg for the optimal solution, compared with 5.5 deg for the linear ap-

proach (Fig. 6b), but it is developed in the first half of the process, and thus, does not have any practical implications. The thrust consumption (Fig. 7) is much smaller for the optimal solution, and its maximum value is only 2.7 N, compared with 6.8 N for the linear model.

The total performance index for the retrieval is 22.2 units, compared with 35.8 units for the linear approach, representing an improvement of 38%. Of this improvement, 15% is due to the new length law and the rest is due to the use of nonlinear terms in the equations. Compared with 23 kg of fuel required with the linear approach, the optimized consumption is only 1.75 kg, which is, of course, a considerable improvement.

#### Four-Segment Massive Tether Model

In the preceding section, the phases of deployment and retrieval were optimized on the basis of the simplified equations of a simple model in which the tether was treated as a massless, straight object. In the present section, the validity of the optimal solution is checked with a more realistic model by using the optimal solution as the nominal path, and using the full nonlinear equations of motion. By comparing the results of the two models, one can ensure that the optimal solution obtained with the simple model is applicable to a more realistic model. In addition, to overcome disturbances and nonzero initial values, and to accommodate the unstable nature of the retrieval process, the system is kept on the nominal path by means of a regulator. Together, the optimal solution is fed forward as the nominal path and a regulator is used to feedback and correct deviations from that nominal path. Because retrieval, unlike deployment,<sup>1</sup> is an unstable process, only retrieval results are presented.

The model now to be used is shown in Fig. 8. The tether is represented by four massless segments, each of length  $L$ , and

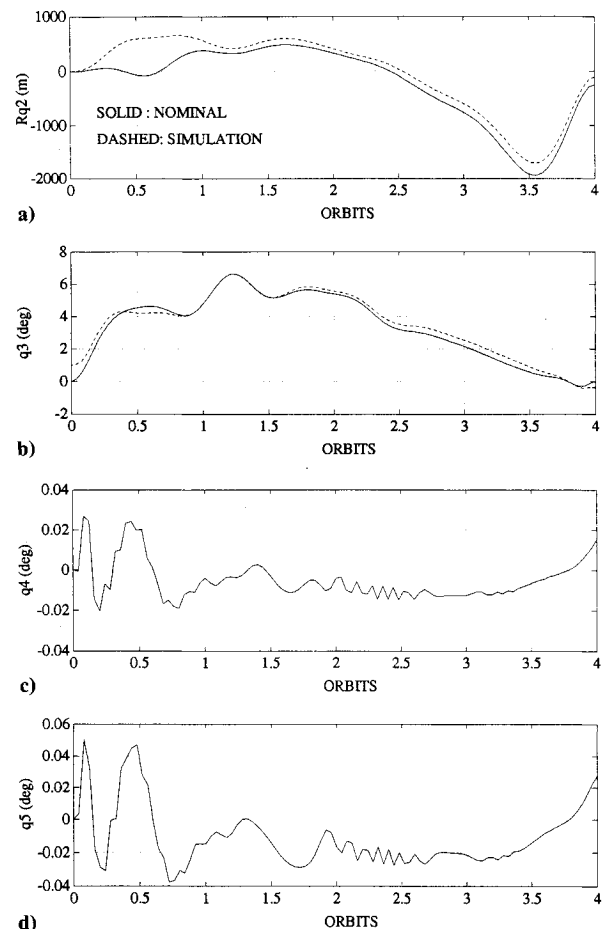


Fig. 9 Retrieval, six-degree-of-freedom model, simulation with full nonlinear equations, and state histories; a) range deviation  $Rq_2$  (m), b)  $q_3$  (deg), c)  $q_4$  (deg), and d)  $q_5$  (deg).

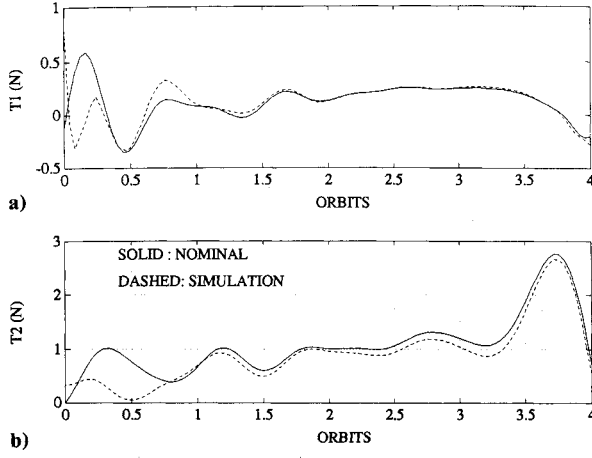


Fig. 10 Retrieval, six-degree-of-freedom model, simulation with full nonlinear equations, and thrust histories (N); a)  $T_1$  and b)  $T_2$ .

three particles, each of mass  $M_T$ . In addition, during deployment and retrieval, the segment lengths vary, and  $M_T$  is expressed as

$$M_T = M_f L / L_f \quad (46)$$

where  $L_f$  and  $M_f$  are the length of one segment and the mass of one particle, respectively, when the tether is fully deployed. The total mass of the system is kept constant by letting the satellite mass  $M$  change in accordance with

$$M = M_s + 1.5(M_f - M_T) \quad (47)$$

where  $M_s$  is the mass of one satellite when the tether is fully extended. To account for the additional tether segments, additional generalized coordinates and the corresponding generalized speeds are introduced. Specifically,  $q_4$ ,  $q_5$ , and  $q_6$  are the bending angles between adjacent tether elements (Fig. 8), and the related generalized speeds are

$$u_i = \frac{dq_i}{d\tau} \quad i = 4, 5, 6 \quad (48)$$

To use the results obtained by the optimization algorithm in a practical manner, the optimal length law that was calculated in the previous section is approximated by a fifth-order polynomial in time

$$L = L_5 t^5 + L_4 t^4 + L_3 t^3 + L_2 t^2 + L_1 t + L_0 \quad (49)$$

where

$$\begin{aligned} L_5 &= 1.325 \times 10^{-17}, & L_4 &= -8.175 \times 10^{-13} \\ L_3 &= 1.792 \times 10^{-8}, & L_2 &= -1.369 \times 10^{-4} \\ L_1 &= -0.4882, & L_0 &= 10,000 \end{aligned} \quad (50)$$

Because the tether is modeled by four segments, which are not accounted for in the optimization procedure, one would expect that bending angles will be excited if the nominal thrusts are used in open loop. Furthermore, it is preferable to operate in closed loop to damp a nonzero initial state vector and other disturbances. Therefore, a regulator is designed to keep the system on the nominal path. The regulator design procedure is the same as in the linear approach; that is, the optimal length law is now considered as prescribed, the equations of motion are linearized, and the LQR technique is used to calculate the feedback gains.

To calculate the regulator feedback gains, we need to write the linearized equations of motion for the model. Before

doing so, we introduce the following dimensionless constants and variables, in addition to those defined in Eqs. (7-12) and (30):

$$\beta = M_T / M \quad (51)$$

$$\hat{u}_i = 10u_i \quad i = 4, 5, 6 \quad (52)$$

$$\hat{q}_i = 10q_i \quad i = 4, 5, 6 \quad (53)$$

The linearized scaled equations of motion are

$$\begin{aligned} (2 + 3\beta)\hat{u}_1' + 0.1(8 + 2\beta)\alpha_f \bar{L}^2 \hat{u}_3 + 0.1(1 + 6\alpha_f + 2\alpha_f \beta) \bar{L} \hat{u}_4' \\ + 0.1(2 + \beta + 4\alpha_f + \alpha_f \beta) \bar{L} \hat{u}_5' + 0.1(1 + 2\alpha_f) \bar{L} \hat{u}_6' \\ + (4 + 6\beta)\hat{u}_2 + 2\bar{L} \Lambda' \{ \alpha_f \bar{L} [(8 + 2\beta) + \alpha_f (8 + 2\beta)] \hat{u}_1 \\ + 0.1(8 + 2\beta)\hat{u}_3 + 0.1(6 + 2\beta)\hat{u}_4 + 0.1(4 + \beta)\hat{u}_5 + 0.2\hat{u}_6 \} \\ + 0.2\hat{u}_4 + 0.2(2 + \beta)\hat{u}_5 + 0.2\hat{u}_6 \} + 0.1\bar{L} \Sigma'' [4\hat{q}_3 + 3\hat{q}_4 \\ + (2 + \beta)\hat{q}_5 + \hat{q}_6] = -(1 + 2\alpha_f \bar{L}) \hat{T}_1 \end{aligned} \quad (54)$$

$$\begin{aligned} (2 + 3\beta)\hat{u}_2' - (4 + 6\beta)\hat{u}_1 - 0.2\bar{L} \hat{u}_4 - 0.1(4 + 2\beta) \bar{L} \hat{u}_5 \\ - 0.2\bar{L} \hat{u}_6 - (6 + 9\beta)\hat{q}_2 - 0.2\alpha_f \bar{L}^2 \Lambda' [\hat{q}_4 + (2 + \beta)\hat{q}_5 \\ + \hat{q}_6] = \hat{T}_2 \end{aligned} \quad (55)$$

$$\begin{aligned} (8 + 2\beta)\alpha_f \bar{L} \hat{u}_1' + 0.1(8 + 2\beta) \bar{L} \hat{u}_3' + 0.1(6 + 2\beta) \bar{L} \hat{u}_4' \\ + 0.1(4 + \beta) \bar{L} \hat{u}_5' + 0.2\bar{L} \hat{u}_6' + 0.1(24 + 6\beta) \bar{L} \hat{q}_3 \\ + 0.1(18 + 6\beta) \bar{L} \hat{q}_4 + 0.1(12 + 3\beta) \bar{L} \hat{q}_5 + 0.6\bar{L} \hat{q}_6 \\ + 2\bar{L} \Lambda' [(8 + 2\beta) + (8 + 2\beta)\alpha_f \hat{u}_1 + 0.1(8 + 2\beta)\hat{u}_3 \\ + 0.1(6 + 2\beta)\hat{u}_4 + 0.1(4 + \beta)\hat{u}_5 + 0.2\hat{u}_6] = -2\hat{T}_1 \end{aligned} \quad (56)$$

$$\begin{aligned} (1 + 2\alpha_f \beta + 6\alpha_f)\hat{u}_1' + 0.1(6 + 2\beta) \bar{L} \hat{u}_3' + 0.1(5 + 2\beta) \bar{L} \hat{u}_4' \\ + 0.1(4 + \beta) \bar{L} \hat{u}_5' + 0.2\bar{L} \hat{u}_6' + 2\hat{u}_2 + 0.1(18 + 6\beta)\hat{q}_3 \\ + 0.1(18 + 6\beta) \bar{L} \hat{q}_4 + 0.1(12 + 3\beta) \bar{L} \hat{q}_5 + 0.6\bar{L} \hat{q}_6 \\ + 2\bar{L} \Lambda' [(6 + 2\beta) + (6 + 2\beta)\alpha_f \hat{u}_1 + 0.1(6 + 2\beta)\hat{u}_3 \\ + 0.1(5 + 2\beta)\hat{u}_4 + 0.1(4 + \beta)\hat{u}_5 + 0.2\hat{u}_6] = -2\hat{T}_1 \end{aligned} \quad (57)$$

$$\begin{aligned} (2 + \beta + 4\alpha_f + \alpha_f \beta)\hat{u}_1' + 0.1(4 + \beta) \bar{L} \hat{u}_3' + 0.1(4 + \beta) \bar{L} \hat{u}_4' \\ + 0.1(4 + \beta) \bar{L} \hat{u}_5' + 0.2\bar{L} \hat{u}_6' + (4 + 2\beta)\hat{u}_2 \\ + 0.1(12 + 3\beta) \bar{L} \hat{q}_3 + 0.1(12 + 3\beta) \bar{L} \hat{q}_4 + 0.1(12 + 3\beta) \bar{L} \hat{q}_5 \\ + 0.6\bar{L} \hat{q}_6 + 2\bar{L} \Lambda' [(4 + \beta) + (4 + \beta)\alpha_f \hat{u}_1 + 0.1(4 + \beta)\hat{u}_3 \\ + 0.1(4 + \beta)\hat{u}_4 + 0.1(4 + \beta)\hat{u}_5 + 0.2\hat{u}_6] = -2\hat{T}_1 \end{aligned} \quad (58)$$

$$\begin{aligned} (1 + 2\alpha_f)\hat{u}_1' + 0.2\bar{L} \hat{u}_3' + 0.2\bar{L} \hat{u}_4' + 0.2\bar{L} \hat{u}_5' + 0.1\bar{L} \hat{u}_6' \\ + 2\hat{u}_2 + 0.6\bar{L} \hat{q}_3 + 0.6\bar{L} \hat{q}_4 + 0.6\bar{L} \hat{q}_5 + 0.6\bar{L}(1 + \alpha_f)\hat{q}_6 \\ + 2\bar{L} \Lambda' (2 + 2\alpha_f \hat{u}_1 + 0.2\hat{u}_3 + 0.2\hat{u}_4 + 0.2\hat{u}_5 + 0.1\hat{u}_6) \\ - 0.1\bar{L} \Sigma'' \hat{q}_6 = -\hat{T}_1 \end{aligned} \quad (59)$$

The regulator is used to keep the system on the nominal path; thus, it is applied to the difference between the actual state vector  $\mathbf{x}$  and optimal state vector  $\mathbf{x}_{nom}$  that has been obtained in the preceding section. Consequently, the control law is

$$\mathbf{v} = \mathbf{v}_{nom} - \mathbf{K}(\mathbf{x} - \mathbf{x}_{nom}) \quad (60)$$

where  $v_{nom}$  is the nominal control history that has been produced by the optimization algorithm and  $K$  is the feedback gains matrix. During deployment and retrieval,  $\bar{L}$ ,  $\beta$ ,  $\Delta'$ , and  $\Delta''$  are time dependent. Consequently, the gain matrix  $K$  also is time dependent. For the purposes of this paper, it is assumed that values of all states can be found at every instant. In reality, this is not the case, and some of the states need to be estimated. The design procedure and performance of such an estimator have been investigated in Ref. 14.

To test the combination of the optimal solution with the regulator, we simulate retrieval with the full nonlinear equations. For the simulation, we take  $M_s = 500$  kg,  $M_f = 164/3 = 54.67$  kg,  $L_f = 5000$  m, and  $t_f = 4$  orbits. The feasibility of the optimal solution for the system under discussion is checked in a realistic manner by simulating retrieval with nonzero initial values, namely  $q_3(0) = 1$  deg. The results of this simulation together with the nominal optimized path are presented in Figs. 9 and 10. The state histories are shown in Fig. 9; it takes the regulator about 1 orbit to converge to the nominal path (Figs. 9a and 9b), and the two solutions remain very close thereafter. The maximum values of the bending angles  $q_4$  and  $q_5$  are 0.03 and 0.05 deg (Figs. 9c and 9d), respectively, which means that the tether remains nearly straight throughout the process. The thrust histories shown in Figs. 10a and 10b show that, once the initial angle has damped out, the consumption is nearly equal to the nominal one. It may be concluded that only a small amount of extra control effort is required to keep the tether straight, and the optimization results are valid for realistic models.

### Conclusion

Results of deployment and retrieval optimization of a tethered satellite system have been presented. The results are applicable to a system that consists of two satellites connected by a tether where one of the satellites is equipped with a set of thrusters. It has been shown that the optimal length law is such that the length changes slowly when the tether is short, and faster when the tether is long. Furthermore, it has been shown that nonlinear terms that include products of thrusts and states cannot be dropped if coordinated thrust actions are expected. The use of optimization algorithms, such as the one used in this paper, enables the designer to put penalties on the terminal values of the states such that at the conclusion of the maneuver the system is near the nominal orbit and the satellites and tether are nearly aligned with the local vertical. The same algorithm might be used for different system parameters, such as tether length, deployment and retrieval time, and orbit altitude, and for elliptic orbits.

Although the optimization analysis is based on a simple model in which the tether is straight and massless, these results are applicable to a more realistic model, one in which the

tether is massive and the first three bending modes are taken into account. The optimal solution obtained with the simple model can be used at the nominal path for the other model, and a regulator can be used to overcome disturbances and unknown initial conditions. It was found that the state and control histories are almost identical for the two systems.

### References

- <sup>1</sup>Netzer, E., and Kane, T. R., "An Alternate Approach to Space Missions Involving a Long Tether," *The Journal of Astronautical Sciences*, Vol. 40, No. 3, 1992, pp. 313-327.
- <sup>2</sup>Misra, A. K., and Modi, V. J., "A Survey on the Dynamics and Control of Tethered Satellite Systems," *Tethers in Space, Advances in the Astronautical Sciences*, Vol. 62, 1986, pp. 667-720.
- <sup>3</sup>Penzo, P. A., and Ammann, P. W., *Tethers In Space Handbook*, Office of Space Flight, NASA Headquarters, Washington, DC, 1989.
- <sup>4</sup>Rupp, C. C., "A Tether Tension Control Law For Tethered Subsatellites Deployed Along Local Vertical," NASA TMX-73314, 1976.
- <sup>5</sup>Vadali, S. R., and Kim, E.-S., "Feedback Control of Tethered Satellites Using Liapunov Stability Theory," *Journal of Guidance, Control, and Dynamics*, Vol. 14, No. 2, 1991, pp. 469-470.
- <sup>6</sup>Bainum, P. M., and Kumar, V. K., "Optimal Control of the Shuttle-Tethered-Subsatellite System," *Acta Astronautica*, Vol. 7, May 1980, pp. 1333-1348.
- <sup>7</sup>Modi, V. J., Chang-Fu, G., Misra, A. K., and Xu, D. M., "On the Control of the Space Shuttle Based Tethered Systems," *Acta Astronautica*, Vol. 9, Nos. 6-7, 1982, pp. 437-443.
- <sup>8</sup>Xu, D. M., Misra, A. K., and Modi, V. J., "Thruster-Augmented Active Control of a Tethered Subsatellite System During Its Retrieval," *Journal of Guidance, Control, and Dynamics*, Vol. 9, No. 6, 1986, pp. 663-672.
- <sup>9</sup>Lakshmanan, P. K., Modi, V. J., and Misra, A. K., "Space Station Based Tethered Payload: Control Strategies and Their Relative Merit," *Tethers in Space Toward Flight*, Third International Conf. on Tethers in Space, AIAA Paper 89-1571-CP, San Francisco, CA, May 1989.
- <sup>10</sup>Fleurisson, E. J., Pines, D. J., and Von-Flotow, A. H., "Trajectory Design, Feedforward and Feedback Stabilization of Tethered Spacecraft Retrieval," AAS/AIAA Spaceflight Mechanics Meeting, AAS Paper 91-176, Houston, TX, Feb. 11-13, 1991.
- <sup>11</sup>Modi, V. J., Lakshmanan, P. K., and Misra, A. K., "Offset Control Strategy for the Space Station Based Tethered Payload," *The Journal of Astronautical Sciences*, Vol. 39, No. 2, 1991, pp. 205-232.
- <sup>12</sup>No, T. S., and Cochran, J. E., "Dynamics and Control of a Tethered Flight Vehicle," AAS/AIAA Astrodynamics Specialist Conf., AAS Paper 91-544, Durango, CO, Aug. 1991.
- <sup>13</sup>Moler, C., Little, J., Bangert, S., and Kleinman, S., *MATLAB User's Manual*, The MathWorks, Inc., Natick, MA, 1985.
- <sup>14</sup>Netzer, E., "An Alternate Approach to Space Missions Involving a Long Tether," Ph.D. Dissertation, Stanford Univ., Stanford, CA, 1992.
- <sup>15</sup>Bryson, A. E., *Control of Spacecraft and Aircraft*, Princeton Univ. Press, Princeton, NJ, 1992 (in press).
- <sup>16</sup>Schaecter, D. B., Levinson, D. A., and Kane, T. K., *AUTOLEV User's Manual*, OnLine Dynamics, Inc., Palo Alto, CA, 1990.